Unsupervised Segmentation of Color Images Based on k-means Clustering in the Chromaticity Plane

L. Lucchese[†‡] and S.K. Mitra[†]
[†]Dept. of Electrical and Computer Eng., University of California, Santa Barbara
[‡]Dept. of Electronics and Informatics, University of Padua, Italy
{luca,mitra}@iplab.ece.ucsb.edu

Abstract

In this work, we present an original technique for unsupervised segmentation of color images which is based on an extension, for an use in the $u'v'$ chromaticity diagram, of the well-known k-means algorithm, widely adopted in cluster analysis. We suggest exploiting the separability of color information which, represented in a suitable 3D space, may be "projected" onto a 2D chromatic subspace and onto a 1D luminance subspace. One can first compute the chromaticity coordinates (u', v') of colors and find representative clusters in such a 2D space, by using a 2D k-means algorithm, and then associate these clusters with appropriate luminance values, by using a 1D k-means algorithm, a simple dimensionally reduced version of the previous one. Experimental evidence of the effectiveness of our technique is reported.

1. Introduction

Cluster analysis represents one of the classical themes of statistical pattern recognition and it has found numerous applications in several fields of image processing; in particular, it has long been used for image segmentation [1, 2]. The early contributions, back to the 70's, mostly dealt with gray-level images and developed many different algorithms to cluster sets of features derived from the intensity information. In more recent times, such techniques have provided a solid basis for multispectral clustering as well; among them, the *k-means algorithm*, originally devised by McQueen [3], is one of the most famous. This algorithm has also been widely used in the fields of vector quantization, where it is known as the *generalized Lloyd algorithm for VQ design* [4], and of data compression, where it is known as the *LBG algorithm* after [5].

The clustering-based techniques for color image segmentation normally choose the RGB space as the feature space (*e.g.*, see [6]-[9] and references therein). A few methods use color spaces other than the RGB; for instance, the CIE $L^*a^*b^*$ color space is preferred in [10]. At any rate, color clustering is generally performed by working in 3D feature spaces, with a few exceptions in which 2D feature spaces are employed [11, 12].

We propose a new procedure that first finds clusters in the 2D plane containing the chromatic information of color and successively associates them with appropriate clusters in the 1D space in which luminance (or brightness) can be represented. An *ad hoc* k-means algorithm can be used, apart from a change of dimensionality, for both these tasks. For the 2D clustering in the $u'v'$ chromaticity plane, we suggest a criterion to adaptively estimate the algorithmic parameters that best suit the data: we show that the distance between each pair of chromaticity coordinates and a baricentric point may be statistically well described by a *Rayleigh probability density function* providing in this way a means for estimating the data spreading. Another feature of our algorithm is that it handles color images in a palettized format; this allows for a very low computational time making our unsupervised segmentation technique suited for real-time applications. The effectiveness of our technique was experimentally tested on several images and here we report on some results.

The organization of the paper is as follows. Section 2 details each step of the algorithm and provides some experimental results. Section 3 draws the conclusions.

2. Segmentation algorithm

2.1. Color representation

For purposes of storage and display, color images are usually represented and handled in the RGB format according to which an image $\mathcal{I}$ may be defined as $\mathcal{I} = \{\mathcal{R}, \mathcal{G}, \mathcal{B}\}$, *i.e.*, as a set of three matrices respectively containing the red, green and blue components of $\mathcal{I}$. In a

0-7695-0034-X/99 $10.00 © 1999 IEEE

Figure 1. A color image $\mathcal{I}$ and its color palette $\mathcal{P}_{RGB}$ with $L = 256$ colors.

palettized format, the image $\mathcal{I}$ is instead represented[1] as $\mathcal{I} = \{\mathcal{Q}, \mathcal{P}_{RGB}\}$, where $\mathcal{Q} \in \mathbb{N}_{[1,L]}^{M \times N}$ is a matrix of pointers to a look-up-table of colors $\mathcal{P}_{RGB} \in \mathbb{R}_{[0,1]}^{L \times 3}$, being L the number of possible combinations of the entries of the three color matrices $\mathcal{R}, \mathcal{G}, \mathcal{B} \in \mathbb{R}_{[0,1]}^{M \times N}$. The color palette $\mathcal{P}_{RGB}$ may be structured as $\mathcal{P}_{RGB} = [\mathbf{R}\ \mathbf{G}\ \mathbf{B}]$, where $\mathbf{R}, \mathbf{G}, \mathbf{B} \in \mathbb{R}_{[0,1]}^{L}$ are, respectively, the vectors containing the red, green and blue coordinates of the possible combinations of colors within the image $\mathcal{I}$. As an example, Fig. 1 shows a color image $\mathcal{I}$ and its color palette $\mathcal{P}_{RGB}$ with $L = 256$ colors. We will also use palette representations in different color spaces; in particular, we represent the palette $\mathcal{P}_{RGB}$ in the XYZ color space as $\mathcal{P}_{XYZ} \doteq [\mathbf{X}\ \mathbf{Y}\ \mathbf{Z}] \in \mathbb{R}_{[0,1]}^{L \times 3}$ through an affine change of coordinates [13].

It is well-known that important color attributes are related to the relative magnitudes of the tristimulus values X, Y and Z (or, equivalently, R, G and B): these quantities are referred to as *chromaticities*. In order to have at disposal an (almost) uniform chromaticity space and easily assess perceptual differences among colors, we have adopted the $u'v'$ diagram in which we represent, in vector form, the chromaticity coordinates of colors as $\mathbf{u'} \doteq 4\mathbf{X}/(\mathbf{X} + 15\mathbf{Y} + 3\mathbf{Z})$ and $\mathbf{v'} \doteq 9\mathbf{Y}/(\mathbf{X} + 15\mathbf{Y} + 3\mathbf{Z})$, $\dim(\mathbf{u'}) = \dim(\mathbf{v'}) = L \times 1$, $(\mathbf{u'}(l), \mathbf{v'}(l)) \in \Upsilon$, $l = 1, \ldots, L$, where quotients between matrices are to be intended as element-wise operations and the symbol $\Upsilon \subset \mathbb{R}^2$ denotes the convex set of the $u'v'$ plane encompassed by the *spectral locus* [13]. Hence, the palette $\mathcal{P}_{XYZ}$ can also be represented, in an equivalent and complete way, as $\mathcal{P}_{u'v'Y} \doteq [\mathbf{u'}\ \mathbf{v'}\ \mathbf{Y}]$.

In the $u'v'$ diagram, one may define two attributes related to hue and saturation of color respectively as $h_{uv} \doteq \arctan((v' - v'_N)/(u' - u'_N))$ and $s_{uv} \doteq 13\sqrt{(u' - u'_N)^2 + (v' - v'_N)^2}$, where u'_N, v'_N are the values of u', v' for a suitably chosen reference white [13]. Fig. 2 shows the $u'v'$ chromaticity diagram (dots) associated with the colors of the image of Fig. 1, along with the spectral locus (solid line) and the reference white (circle), selected as the standard illuminant D_{65} ($u'_N = 0.1978$ and $v'_N = 0.4683$).

[1] Throughout the text, the notation $\boldsymbol{A} \in \mathbb{S}_{[\alpha,\beta]}^{M \times N}$ indicates that each element a_{ij} of the matrix $\boldsymbol{A} \in \mathbb{S}^{M \times N}$ takes values in the set $[\alpha, \beta] \subset \mathbb{S}$.

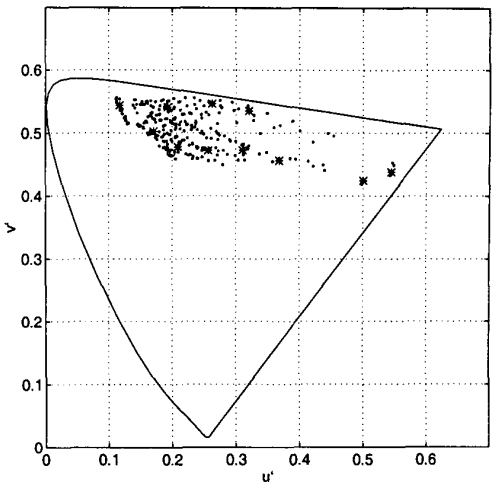

Figure 2. Chromaticity diagram $u'v'$ (dots) relative to the colors of the image of Fig. 1 and set of cluster seeds $\mathbb{K} = \{\kappa_n\}_{n=1,\ldots,N}$, $N = 11$, (asterisks).

2.2. 2D k-means clustering in the $u'v'$ chromaticity plane

Our goal is to find the most representative clusters in the chromaticity diagram, since they contain the great part of the information associated with the main color families within an image. Hunt in [14] observes that hue and saturation are the color attributes which turn out to be the most invariant to changes due to surface curvature of colored objects and lighting conditions. Therefore, to single out the main homogeneous color regions within an image, we search for clusters of hue and saturation by working in the Cartesian coordinates (u', v'). These clusters can be easily found by means of an *ad hoc* extension of the *k-means algorithm* [1]; a sketch of our implementation of this algorithm is reported in Fig. 3.

This algorithm lends itself to the following comments. First of all, it requires only one iteration; the number of clusters changes during the clustering process and we do not know *a priori* the number of clusters we will end up with. When a point must be associated with a cluster or two cluster seeds must be merged together, a *center of gravity law* is adopted; in this way, the outcoming seed is closer

▷ from $\mathcal{Q}$, compute the normalized distribution vector $\boldsymbol{w} \in \mathbb{Q}^{L}_{[0,1]}$, $\| \boldsymbol{w} \| = 1$, containing the number of pixels per each entry in the color palette $\mathcal{P}_{u'v'Y}$;
▷ compute the baricenter of the data in the $u'v'$ plane as $\boldsymbol{v}_\beta = (u'_\beta, v'_\beta) \in \Upsilon$, with $u'_\beta \doteq \boldsymbol{w}^T \mathbf{u}'$ and $v'_\beta \doteq \boldsymbol{w}^T \mathbf{v}'$;
▷ sort the vector $\boldsymbol{w}$ in descending order and define the vector $\boldsymbol{p} \in \mathbb{N}^{L}_{[1,L]}$ containing such ordering;
▷ set $\boldsymbol{v}_\beta$ as the initial seed for clustering in the $u'v'$ space, associate it with a weight $w_\beta = 0$, and initialize with them, respectively, two ordered sets $\mathbb{K} \subset \Upsilon$ and $\mathbb{W}_K \subset \mathbb{Q}_{[0,1]}$ whose elements are dinamically ordered according to their insertion or extraction order;
`for` $l = 1$ `to` $l = L$
  ▷ define $\boldsymbol{v}(l) \doteq (\mathbf{u}'(\boldsymbol{p}(l)), \mathbf{v}'(\boldsymbol{p}(l))) \in \Upsilon$;
  ▷ compute the minimum distance $d(i)$ between $\boldsymbol{v}(l)$ and the cluster seeds in the set $\mathbb{K}$ as $d(i) = \min_{\boldsymbol{\kappa} \in \mathbb{K}} \| \boldsymbol{v}(l) - \boldsymbol{\kappa} \|$;
  let $\boldsymbol{\kappa}(i) \in \mathbb{K}$ denote the closest seed;
  `if` $d(i) > \tau_1$
  `then`
    ▷ add $\boldsymbol{v}(l)$ to the set $\mathbb{K}$ as a new seed and its associated weight $\boldsymbol{w}(\boldsymbol{p}(l))$ to the set $\mathbb{W}_K$;
  `else`
    ▷ $\boldsymbol{v}(l)$ belongs to the cluster defined by $\boldsymbol{\kappa}(i)$; this induces the shifting of the seed $\boldsymbol{\kappa}(i)$ whose new position and associated weight are respectively updated as

$$\boldsymbol{\kappa}(i) := \frac{w_{\boldsymbol{\kappa}}(i)\boldsymbol{\kappa}(i) + \boldsymbol{w}(\boldsymbol{p}(l))\boldsymbol{v}(l)}{w_{\boldsymbol{\kappa}}(i) + \boldsymbol{w}(\boldsymbol{p}(l))} \quad \text{and} \quad w_{\boldsymbol{\kappa}}(i) := w_{\boldsymbol{\kappa}}(i) + \boldsymbol{w}(\boldsymbol{p}(l));$$

    ▷ compute the minimum distance $d(j)$ between $\boldsymbol{\kappa}(i)$ and the other seeds in $\mathbb{K}$ as $d(j) = \min_{\substack{\boldsymbol{\kappa} \in \mathbb{K} \\ \boldsymbol{\kappa} \neq \boldsymbol{\kappa}(i)}} \| \boldsymbol{\kappa}(i) - \boldsymbol{\kappa} \|$;
    `if` $d(j) < \tau_2$
    `then`
      ▷ the clusters associated with the seeds $\boldsymbol{\kappa}(i)$ and $\boldsymbol{\kappa}(j)$ must be merged together and the position and weight of the new resulting cluster are computed according to the following procedure:
      ▷ define $m \doteq \min(i, j)$ and $M \doteq \max(i, j)$;
      ▷ update

$$\boldsymbol{\kappa}(m) := \frac{w_{\boldsymbol{\kappa}}(i)\boldsymbol{\kappa}(i) + w_{\boldsymbol{\kappa}}(j)\boldsymbol{\kappa}(j)}{w_{\boldsymbol{\kappa}}(i) + w_{\boldsymbol{\kappa}}(j)} \quad \text{and} \quad w_{\boldsymbol{\kappa}}(m) := w_{\boldsymbol{\kappa}}(i) + w_{\boldsymbol{\kappa}}(j);$$

      ▷ remove the seed $\boldsymbol{\kappa}(M)$ from $\mathbb{K}$ and its weight $w_{\boldsymbol{\kappa}}(M)$ from $\mathbb{W}_K$;
    `end`
  `end`
`end`

Figure 3. Algorithm for 2D k-means clustering in the $u'v'$ chromaticity plane.

to the "heaviest" of the two points, that is, to the point which, in the chromaticity plane, represents the color entering the highest percentage of pixels. Moreover, our procedure spans the points from the "heaviest" to the "lightest" so that, after the first iterations, the seeds do not move significantly, since the early formed seeds are rather "heavy". The fact that we choose only one initial seed instead of many does not affect the performance of the algorithm [1]. On the contrary, the two parameters which significantly affect the clustering process are the threshold parameters τ_1 and τ_2 (see Fig. 3), and they are to be carefully selected since they determine to a broad extent the final number of colors (phases) in the segmented image.

The parameter τ_1 determines the average distance among clusters whereas the parameter τ_2 is related to the average radius of the clusters, regarding them as circles. In order to get an estimate of τ_1, we need to have an idea of the spreading of the data in the $u'v'$ plane. In fact, different images can give rise to very different constellations of points in the chromaticity plane, and consequently to very different average inter-cluster distances. Thus it is not possible to set a value of τ_1 good for any image which is a data-dependent parameter to be retailed on the specific image; however, an estimate of τ_1 may be readily derived as follows. Let us consider the probability function $F(x) \doteq P[\| \boldsymbol{v} - \boldsymbol{v}_\beta \| \leq x]$, $\boldsymbol{v}, \boldsymbol{v}_\beta \in \Upsilon$, $x \geq 0$, which describes the distribution of the distance between each point $\boldsymbol{v}$ and the baricenter $\boldsymbol{v}_\beta$ of the data (see Fig. 3); it is well-known that, if these points were Gaussian distributed around $\boldsymbol{v}_\beta$, the probability density function $f(x) \doteq dF(x)/dx$ would be the *Rayleigh density function* $f(x) = (x/\sigma^2)e^{-x^2/2\sigma^2}h(x)$, where $h(x)$ is the unit-step function [15]. Although real imagery usually does not generate Gaussian distributed points in the chromaticity plane, we could experimentally ascertain that a *Rayleigh density function* may describe fairly well the statistical distribution of the data. In practice, we compute the (discrete)

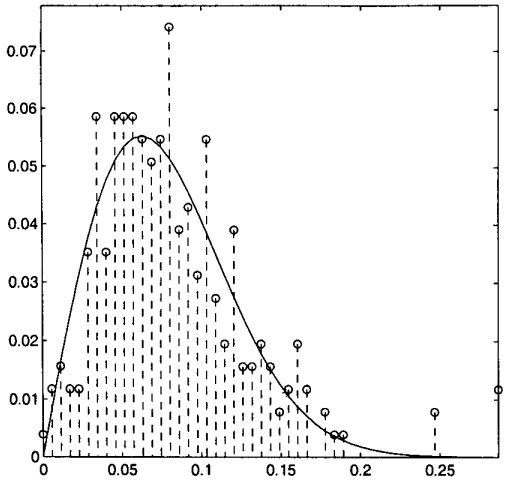

Figure 4. Frequency histogram $\mathcal{H}(d(l))$ (dashed bars) and fitting function $g(x)$ (solid line).

distance function $d(l) \doteq \| \boldsymbol{v}(l) - \boldsymbol{v}_\beta \|, l = 1, \ldots, L$, and we fit its frequency histogram $\mathcal{H}(d(l))$ (50 bins) with the continuous function $g(x) = cf(x)$, where the coefficient c accounts for the bias of the data; the fitting is performed via a standard non-linear least square algorithm. Fig. 4 shows the histogram $\mathcal{H}(d(l))$ (dashed bars) and the function $g(x)$ (solid line). It can be seen that the fitting of the data is rather good. The probability function $f(x)$ allows us to estimate the radius ϱ_ω of the circle in which a certain percentage ω of the data ($0 \leq \omega \leq 1$) is contained; such radius is given by $\varrho_\omega = \sigma\sqrt{2\ln(1/(1-\omega))}$; in our experimental setup, we have chosen $\omega = 0.95$. Experimentally, we have found out that setting $\tau_1 = \varrho_\omega/4$ and $\tau_2 = \varrho_\omega/8$ gives excellent segmentation result with a wide variety of color images; this choice produces a limited number of segments (usually, less than 20) which well represent the chromatic information of images. Of course, one might decide to supervisedly reduce (increase) the number of segments by increasing (reducing) τ_1, always as a fraction of ϱ_ω, since this parameter captures the spreading of data in the chromaticity plane. The parameter τ_2 may be freely set with the only constraint that $\tau_2 < \tau_1$ to prevent cluster overlapping.

2.3. 1D k-means clustering for the luminance Y

The previous step of the algorithm returns a set of cluster seeds $\mathbb{K} = \{\boldsymbol{\kappa}_n\}_{n=1,\ldots,N}$ defining the main colors within the image $\mathcal{I}$ only by means of their coordinates (u', v'). In Fig. 2, the asterisks represent the cluster seed set $\mathbb{K}$ ($N = 11$) found by the algorithm of Fig. 3. For a complete characterization of colors, we need now to relate the chromaticity coordinates with suitable values of luminance Y. To this end, we consider the sets $\mathcal{Y}_n \doteq \{\mathbf{Y}(l) \in \mathbb{R}_{[0,1]} :$

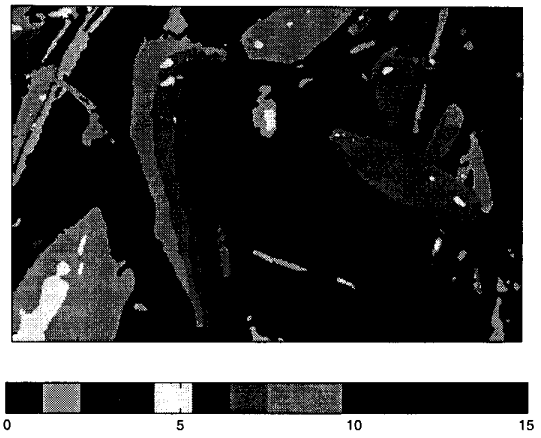

Figure 5. Segmented image $\mathcal{I}^S$ and its color palette $\mathcal{P}^S_{RGB}$ with $S = 14$ colors after median filtering.

$\| \boldsymbol{v}(l) - \boldsymbol{\kappa}_n \| \leq \tau_2, \boldsymbol{v}(l) \in \Upsilon, l = 1, \ldots, L, \boldsymbol{\kappa}_n \in \mathbb{K}\}$, $n = 1, \ldots, N$, which encompass the luminance values associated with the points $\boldsymbol{v}(l)$ contained in circles centered at the cluster seeds $\boldsymbol{\kappa}_n$ and having radius τ_2. To the sets $\mathcal{Y}_n, n = 1, \ldots, N$, we apply a 1D k-means clustering algorithm which consists in a simple dimensional reduction of the 2D algorithm of Fig. 3. The thresholds τ_3 and τ_4 which respectively play the 1D counterpart of τ_1 and τ_2 have been experimentally chosen as $\tau_3 = 0.5$ and $\tau_4 = 0.2$. This choice is motivated by the adopted normalization of the luminance between 0 and 1. In fact, as τ_3 determines the inter-cluster distance, it has been set equal to half the scale range in order not to generate too many segments; τ_4 determines instead the intra-cluster spreading and it has to satisfy the constraint $\tau_4 < \tau_3$ to prevent cluster overlapping as in the 2D case. However, the selection of such 1D thresholds is not so crucial as that of the 2D thresholds reported in Section 2.2, since rather wide changes of τ_3 and τ_4 yield not appreciably different segmentation results.

2.4. Palette color matching and post-processing

At the end of the 1D k-means algorithm applied to the luminance $\mathbf{Y}$, we obtain a certain number S of representative points in the $u'v'Y$ space; they are ordered into a color palette according to increasing values of hue-angle. This palette is converted into XYZ coordinates and successively into RGB coordinates as $\mathcal{P}^S_{RGB} \in \mathbb{R}^{S\times 3}_{[0,1]}$. The color matching procedure of [16] in the $L^*u^*v^*$ space is then applied to $\mathcal{P}_{RGB}$ and $\mathcal{P}^S_{RGB}$ and, by rearranging the indexing of $\mathcal{Q}$ with respect to the new color palette, we finally obtain the segmented image $\mathcal{I}^S$ expressed in a palettized format as $\mathcal{I}^S = \{\mathcal{Q}^S, \mathcal{P}^S_{RGB}\}$. However, this operation usually yields a number of very small regions which can be elimi-

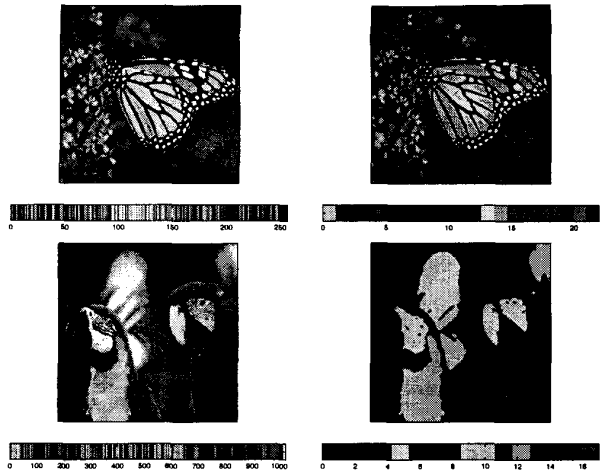

Figure 6. Some other segmentation results.

nated with a scalar median filtering applied to $\mathcal{Q}^S$; the color ordering of $\mathcal{P}^S_{RGB}$ hinders median filtering from introducing false colors. The resulting image is plotted in Fig. 5; as expected, our algorithm returns rather homogeneous regions even in the presence of changes of color appearance caused by surface curvature of objects and by slight shadowing. Similar results were obtained with other color images as well (see Fig. 6). The algorithm turns out to be deceived in correspondence of the surface patches affected by highlighting, mutual reflections and dark shadows. In order to prevent these artifacts though, one should resort to physics-based segmentation algorithms which make use of complicated hypotheses on the interaction between light and objects in a scene.

3. Conclusions

We have presented a novel technique, based on cluster analysis, for segmentation of color images. We have suggested dividing the problem of color segmentation, intrinsically 3D, into two parts. In the first part, only the chromatic information is segmented by using a 2D k-means algorithm in the $u'v'$ plane; in the second part, the chromaticity clusters are associated with appropriate intensity values through the 1D version of the k-means algorithm used in the first part. A statistical criterion to adaptively taylor the algorithm on the data has been proposed too. Experimental evidence of the effectiveness of our technique has been reported.

Acknowledgements

This work was supported in part by C.N.R., Italy, through a fellowship for research abroad (n. 203.15.9) and in part by a University of California MICRO grant, with matching supports from Lucent Technologies, Raytheon Missile Systems, Tektronix Corp. and Xerox Corp.

References

[1] M.R. Anderberg, *Cluster Analysis for Applications*, Academic Press, New York, NY, 1973.

[2] G.B. Coleman and H.C. Andrews, "Image Segmentation by Clustering," *Proc. of the IEEE*, Vol. 67, No. 5, pp. 773-785, May 1979.

[3] J. McQueen, "Some Methods for Classification and Analysis of Multivariate Observations," *Proc. of the* 5^{th} *Berkeley Symp. on Math. Stat. and Prob.*, Vol. 1, pp. 281-296, 1967.

[4] A. Gersho and R.M. Gray, *Vector Quantization and Signal Compression*, 4^{th} Ed., Kluwer Academic Press, Boston, MA, 1995.

[5] Y. Linde, A. Buzo, and R.M. Gray, "An Algorithm for Vector Quantizer Design," *IEEE Trans. Comm.*, COMM-28, pp. 84-95, Jan. 1980.

[6] D. Comaniciu, P. Meer, "Robust Analysis of Feature Spaces: Color Image Segmentation," *Proc. of CVPR'97*, pp. 750-755.

[7] W.P. Berriss, S.J. Sangwine, "A Colour Histogram Clustering Technique for Tissue Analysis of Healing Skin Wounds," *Proc. of* 6^{th} *Int'l Conf. on Image Proc. and Its Appl.*, Vol. 2, pp. 693-697, July 1997.

[8] H.C. Yung, H.S. Lal, "Segmentation of Color Images Based on the Gravitational Clustering Concept, " *Optical Engineering*, Vol. 37, No. 3, pp. 989-1000, Mar. 1998.

[9] S.H. Park, I.D. Yun, S.U. Lee, "Color Image Segmentation Based on 3-D Clustering: Morphological Approach," *Pattern Recognition*, Vol. 31, No. 8, pp. 1061-1076, Aug. 1998.

[10] W. Woelker, "Image Segmentation Based on an Adaptive 3D Analysis of the CIE-$L^*a^*b^*$ Color Space," *Proc. of SPIE'96 - Visual Communications and Image Processing '96*, Vol. 2727, pp. 1197-1203, 1996.

[11] P. Schmid, S. Fischer, "Colour Segmentation for the Analysis of Pigmented Skin Lesions," *Proc. of* 6^{th} *Int'l Conf. on Image Proc. and Its Appl.*, Vol. 2, pp. 688-692, July 1997.

[12] J. Luo, R.T. Gray, H.C. Lee, "Towards Physics-based Segmentation of Photographic Color Images", *Proc. of ICIP'97*, Vol. III, pp. 58-61.

[13] R.W.G. Hunt, *Measuring Colour*, 2^{nd} Ed., Ellis Horwood Ltd. Publ., Chichester, UK, 1987.

[14] R.W.G. Hunt, *The Reproduction of Colour*, 5^{th} Ed., Fountain Press, Kingstone-upon-Thames, UK, 1995.

[15] H. Stark and J.W. Woods, *Probability, Random Processes, and Estimation Theory for Engineers*, 2^{nd} Ed., Prentice Hall, Englewood Cliffs, NJ, 1994.

[16] L. Lucchese and S.K. Mitra, "An Algorithm for Fast Segmentation of Color Images," to appear in *Proc. of the* 10^{th} *Int'l Tyrrhenian Workshop on Digital Communications - "Multimedia Communications,"* Ischia, Italy, Sept. 1998.